

Antenna Measurement Range Characterization and Compensation (A Remembrance)

Ed Joy, Professor Emeritus
Georgia Institute of Technology

This paper is a remembrance of the research conducted over the period 1987 – 2001 at the Georgia Institute of Technology to compensate measured antenna patterns made on fixed-line-of-sight far-field, anechoic chamber, compact or spherical near-field antenna measurement ranges for measured imperfections in the amplitude, phase and polarization of the test-zone fields of these antenna ranges.

Range Characterization

The most common far-field, anechoic chamber and compact range characterization method used in the 1970s and 1980s was the linear probe scanner. The scanner moved a linearly polarized, 10 – 15 dB_i gain antenna as the probe antenna, along a line across the test zone and perpendicular to the range axis. The probe antenna boresight direction was aligned parallel to the range axis. The range axis is the line that connects the center of rotation of the Antenna Under Test (AUT) and the center of rotation of the range antenna. Several cuts of the test zone were made. Most commonly, horizontal and vertical cuts were made. Cuts were made for the probe horizontally polarized and repeated for the probe vertically polarized. Occasionally cuts were also made in the $\pm 45^\circ$ planes and occasionally circularly polarized probes were used instead of linearly polarized probes. Scientific-Atlanta (SA) sold a linear scanner especially designed for this purpose. The SA scanner incorporated a small roll positioner to which the probe antenna could be mounted. This roll positioner allowed the selection of the probe linear polarization direction. The SA scanner was commonly mounted on the existing range AUT roll positioner such that the scanning direction could be easily selected. Later Near-Field Systems (NSI) made a “half scanner” which was also mounted on a roll positioner, but scanned the radius of the test zone rather than the diameter. The linear scanner allowed measurement of the amplitude, phase, and polarization of the field entering the test zone from the direction of the range antenna and from perhaps $\pm 45^\circ$ from the range axis. The $\pm 45^\circ$ capture angle was normally sufficient to capture range antenna pattern reflections from the ground on a far

field range; wall, ceiling and floor reflections on an anechoic chamber and edge scattering on a compact range. The linear scanner did not capture wide angle reflections or reflections from behind the test zone.

Spherical test-zone probing was an obvious solution to measuring all the fields entering a spherical test zone. The fields measured on a spherical surface enclosing a spherical test zone using an outward directed probe are difficult to display and sometimes difficult to understand. From spherical test-zone field probing it was difficult to see amplitude and phase taper and polarization anomalies that were much easier to see using linear probing data. The probe used for spherical probing has similar requirements to the probe used in linear probing, but has a further requirement of requiring a high front-to-back pattern ratio. This high front to back ratio is important when measuring very low amplitude fields entering the rear of the test zone while the high amplitude main beam of the range antenna is entering the rear of the test-zone probe. Often an absorbing baffle is used to further increase the front-to-back ratio of the spherical probe. The angular spectrum of the fields entering the sphere is extremely helpful in identifying the quality of the test-zone field amplitude, phase and polarization and the directions to areas and objects of reflection and location of leaking cables and equipment within the range.

Standard spherical mode spectrum mathematics is used to calculate the spherical mode spectrum of the spherical surface test-zone fields, but the standard spherical mathematics was developed for spherical near-field measurement and used outward propagating spherical modes. Spherical test-zone measurement requires measurement of inward propagating modes and also requires measurement and characterization of standing-wave modes. Thus, a reformulation of the calculation of the spherical modal spectrum was required. Determination of the spherical modal spectrum of the spherical surface fields is much simpler if the probe is cylindrically symmetric, with a primary polarization mode of $\mu = \pm 1$. A circular open-ended wave guide satisfies these conditions and can be used for a spherical surface probe, whether pointed into the sphere for spherical near-field measurements or out of the sphere for measuring incoming fields. A rectangular open-ended waveguide is often used but does not have the cylindrical symmetry of the cylindrical open-ended waveguide and does not have the polarization mode of $\mu = \pm 1$. The angular sampling spacing requirement for range characterization is $\leq \lambda/(2r_0)$ radians in both spherical directions, where r_0 is the radius of the test-zone sphere. The corresponding maximum spatial sample spacing is $\lambda/2$ which occurs

on the equator of the sphere of radius r_0 . Near the poles of the sphere the spatial sample spacing is much less. The $\lambda/2$ spatial sampling spacing is sufficient as the test-zone fields should be totally radiating fields.

A measurement demonstration was undertaken and the following is the result. The Georgia Tech Spherical Near-field/Far-field range was reconfigured as a spherical surface test-zone measurement system. This required conversion of the polar roll over azimuth spherical AUT positioning system to an equatorial spherical outward-looking probe positioning system. Figure 1. Shows the outward looking probe, the rotary joint for polarization rotation and the absorber shield used to significantly reduce the back pattern amplitude of the probe. The conversion from a polar positioning system to an equatorial positioning system is simply the use of a 90° bend on the roll (head) positioner. This conversion is not conceptually difficult; however, it was found that the structure as shown in Figure 1 needed to be more mechanically robust. Figures 2 and 3 show the next generation probe support and positioner, which has been used ever since.

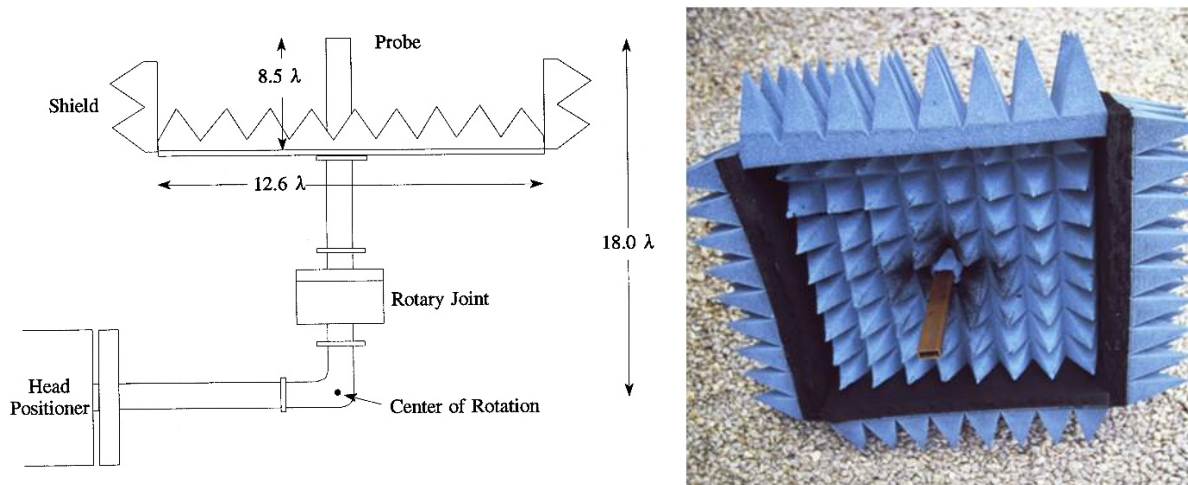


Figure 1. Open-ended rectangular waveguide test-zone field probe with absorber shield and rotary joint equatorially mounted on roll (head) over azimuth positioner

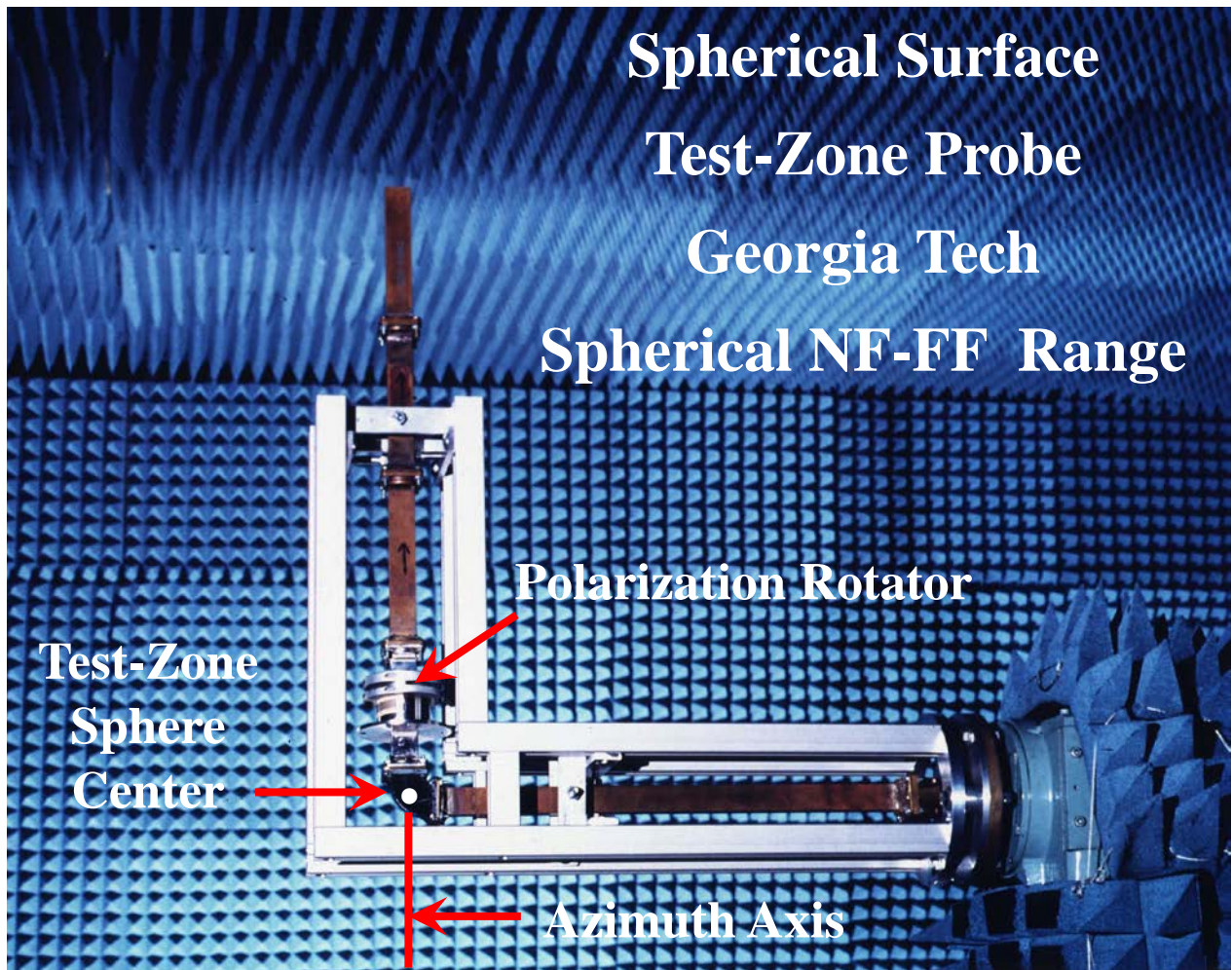


Figure 2. Probe support structure and polarization rotator for an open-ended rectangular waveguide probe mounted on the head (roll) positioner, shown without absorber

The spherical test-zone probe shown in Figure 2 has a spherical radius of 58 cm which equals 18λ at 9.33 GHz. Thus, the measurement sphere has a diameter of 116 cm or 36λ . The spherical test-zone probe system was designed to eventually measure an elliptical flat-plate array antenna with aperture dimensions of 71.7 cm x 65.26 cm. The spherical test-zone probe system of Figure 2 comfortably houses the intended AUT with a spacing of at least 6.9λ all around the AUT. This new equatorially mounted probe test-zone characterization system was used to measure the spherical test zone of the range configuration shown in Figure 4. Note in Figure 4, in addition to the field produced by the range antenna there are two major reflectors in the range.

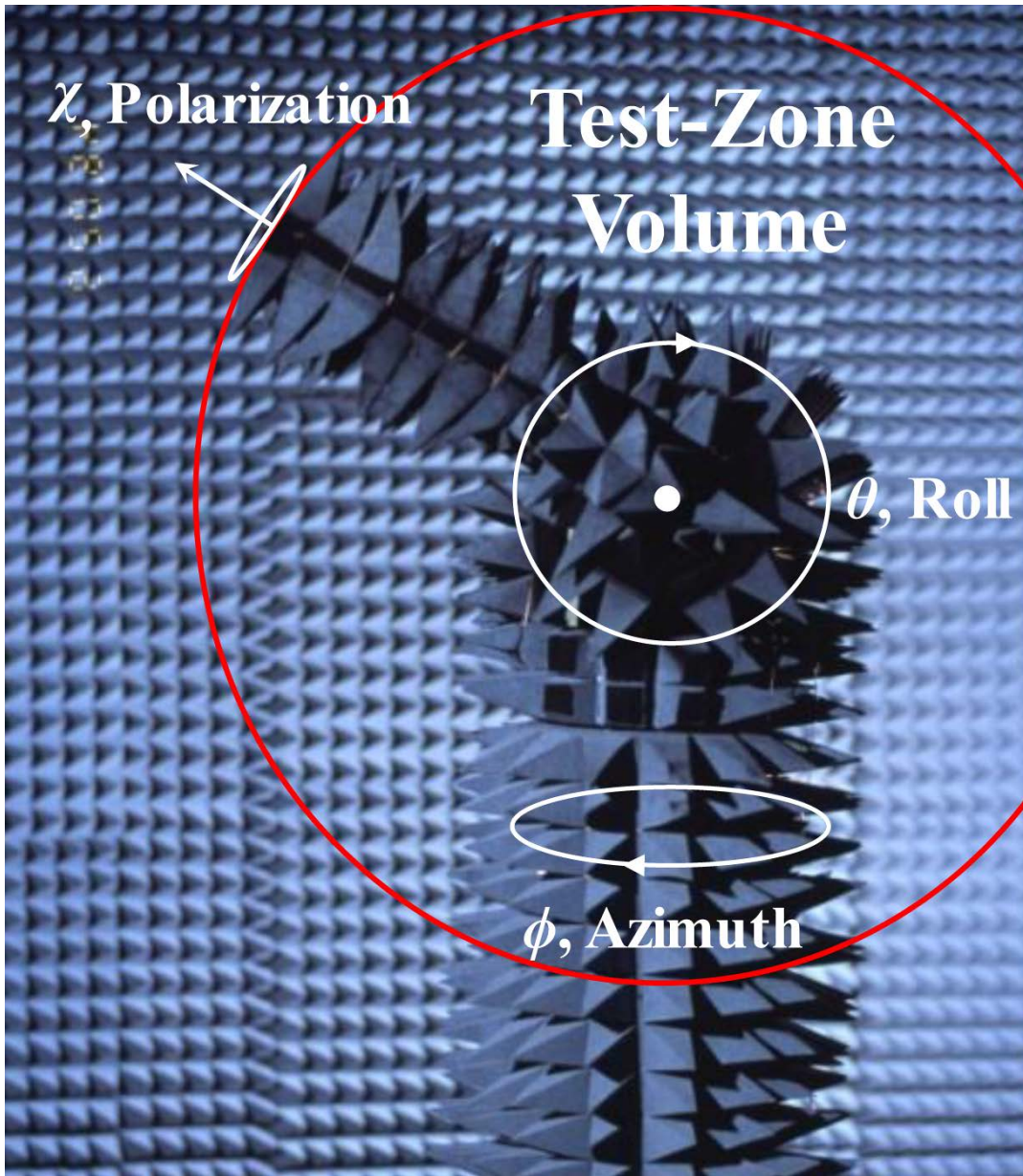


Figure 3. Absorber wrapped open-ended rectangular-waveguide probe, probe support structure and probe rotation diagrams in phi (azimuth), theta (roll) and chi (polarization). Everything within the test-zone volume is covered with absorber.

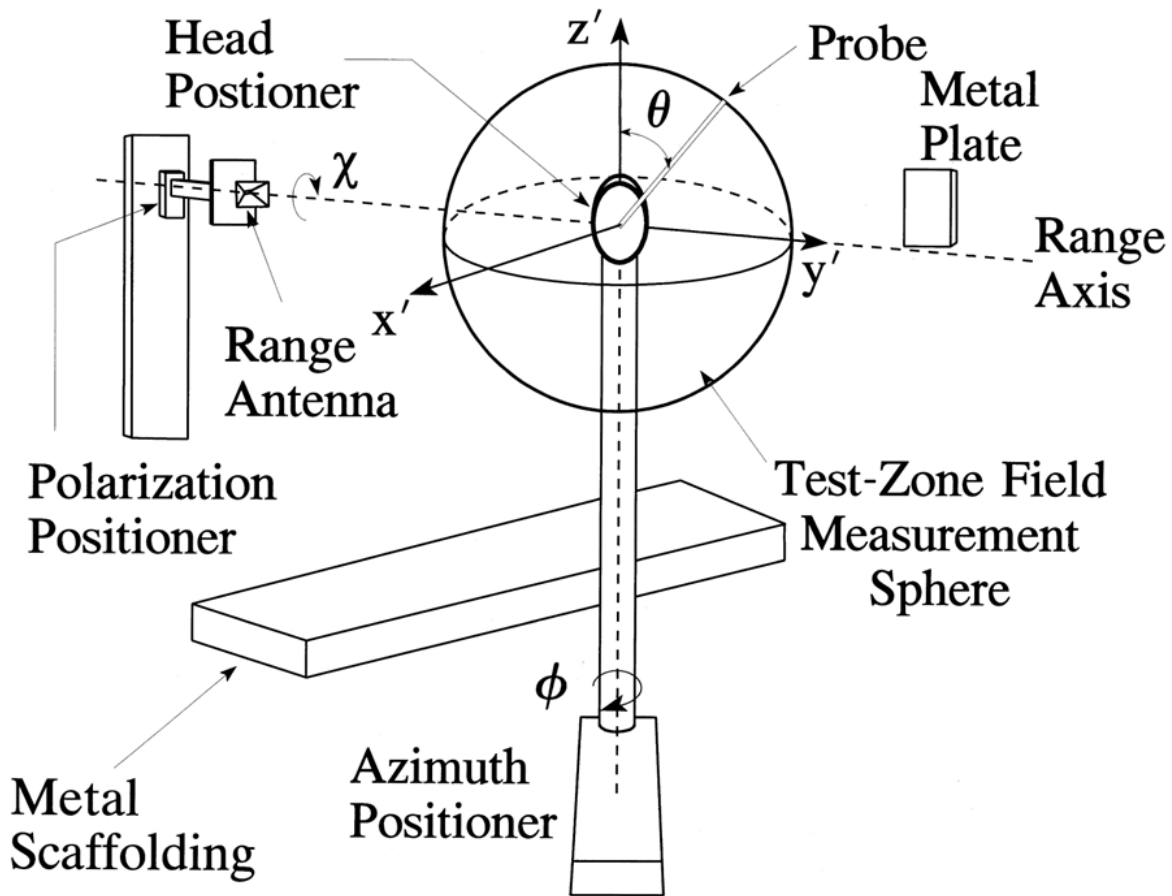


Figure 4. Georgia Tech Near-field/Far-field range with range antenna, a metal plate and a metal scaffolding used as reflectors. The test-zone measurement sphere and probe are shown.

The two spherical surface test-zone measurements, one for the range antenna vertically polarized and one after a 90° roll rotation of the range antenna to produce a horizontally polarized range antenna are shown in Figure 5. Figure 5 shows the approximate location of the two metal reflectors and clearly shows the effect of the reflections on the test-zone fields for both polarizations. The entire test-zone field is rotated when the range antenna is rotated. It is often thought that rotating the range antenna simply rotates the polarization of the test-zone field. The test-zone fields rotate while the reflectors and associated reflections do not. There are two very different test-zone fields, not simply a single test-zone field with a change of polarization.

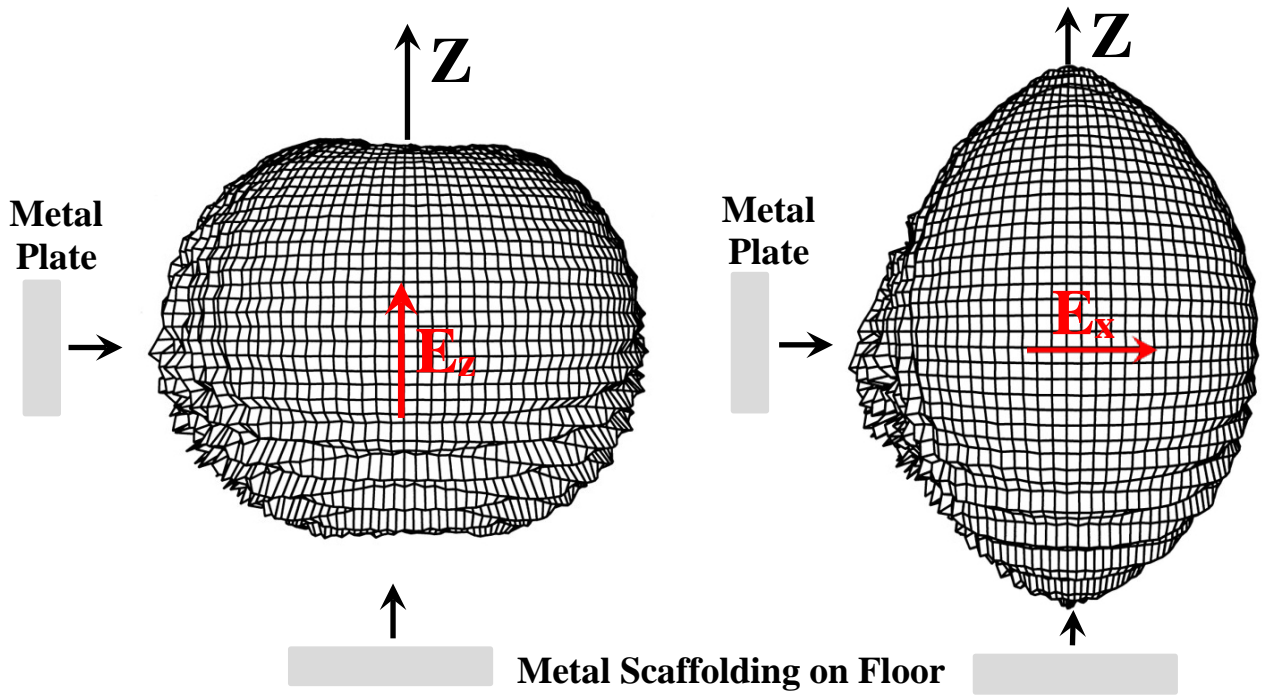


Figure 5. Spherical surface test-zone field measurement for two polarizations of the range antenna in the presence of two reflectors.

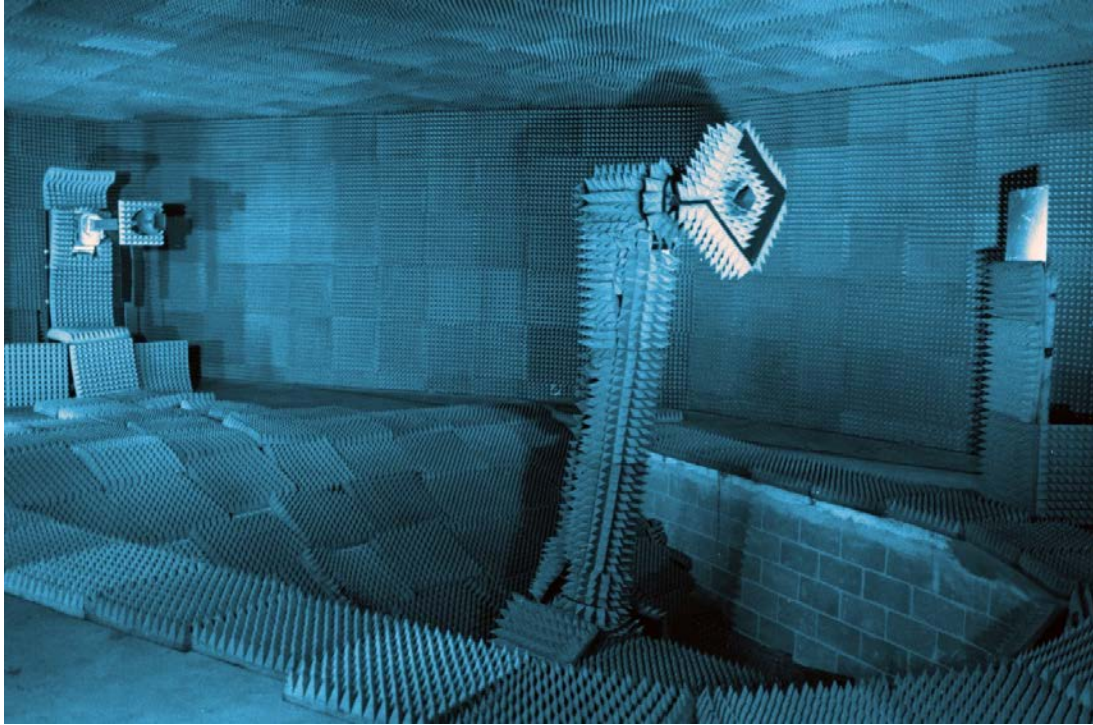


Figure 6 is a photograph of the reconfigured spherical positioning system and chamber for measurement of an AUT. The AUT shown is a small horn antenna. An absorbing shield, once used as a probe shield is being used as a shield for the AUT measurement. A flat plate reflector is located at approximately 135° in azimuth, where 0° is the azimuth location of the range antenna.



Richard Wilson

Richard Wilson, Chief Engineer of the Georgia Tech Near-field/Far-field Antenna Measurement Range, calculated the field inside, the assumed to be vacant test-zone sphere, from the field measured on the surface of the sphere. Figure 7 shows the calculated field on the principal horizontal plane inside the measurement sphere of the range shown in Figure 6. A similar calculation of the field on a vertical plane located within the test zone, with the perpendicular to the plane pointing toward the range antenna, could be made. The calculated field on a vertical plane could be used to easily quantify the amplitude and phase taper and ripple. The polarization purity of the test-zone field could be determined as carried out for linear or planar probing. Thus, linear or planar probing apparatus can be replaced with spherical probing apparatus and associated software.

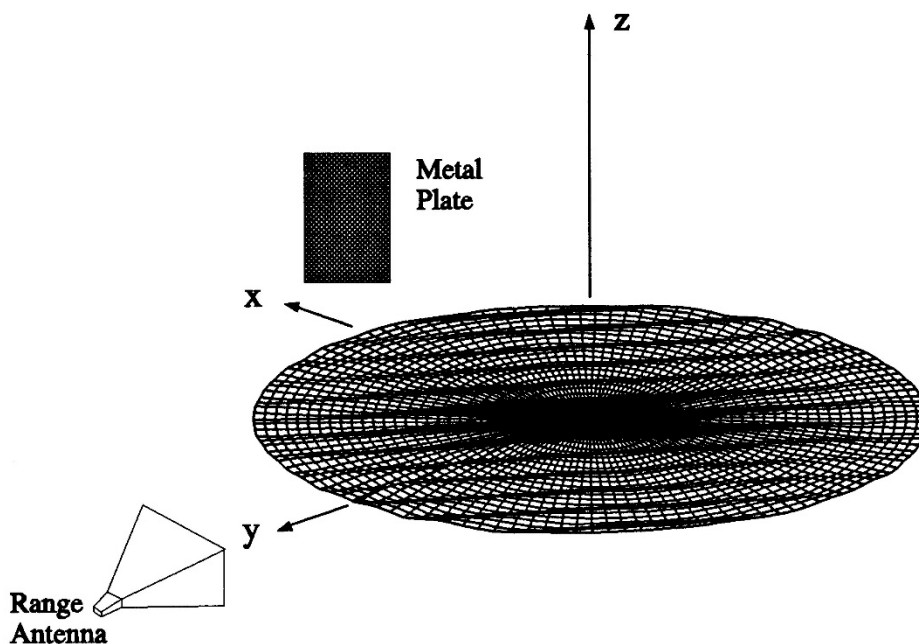


Figure 7. The test-zone field amplitude calculated on the center horizontal plane of the spherical test zone of the range in Figure 6. The interference between the field from the range antenna and the field reflected from the metal plate is shown.

Ron Wittmann and Mike Francis of NIST became interested in range characterization and had a long history of working with spherical near-field systems and software. They developed, used, and extended the NIST spherical test-zone software for imaging antenna measurement ranges. Figure 8 is a photograph of the NIST Cylindrical/Spherical near-field range in the spherical configuration. The photo shows that Mike parked his bike in the range, which in this case is being used as a reflector. Figure 9 show a portion of the image of the range which includes Mike's bike. The image is recognizable as a bicycle. The spherical test-zone sphere has a radius of 64 cm and the measurement frequency was 16 GHz for this measurement.

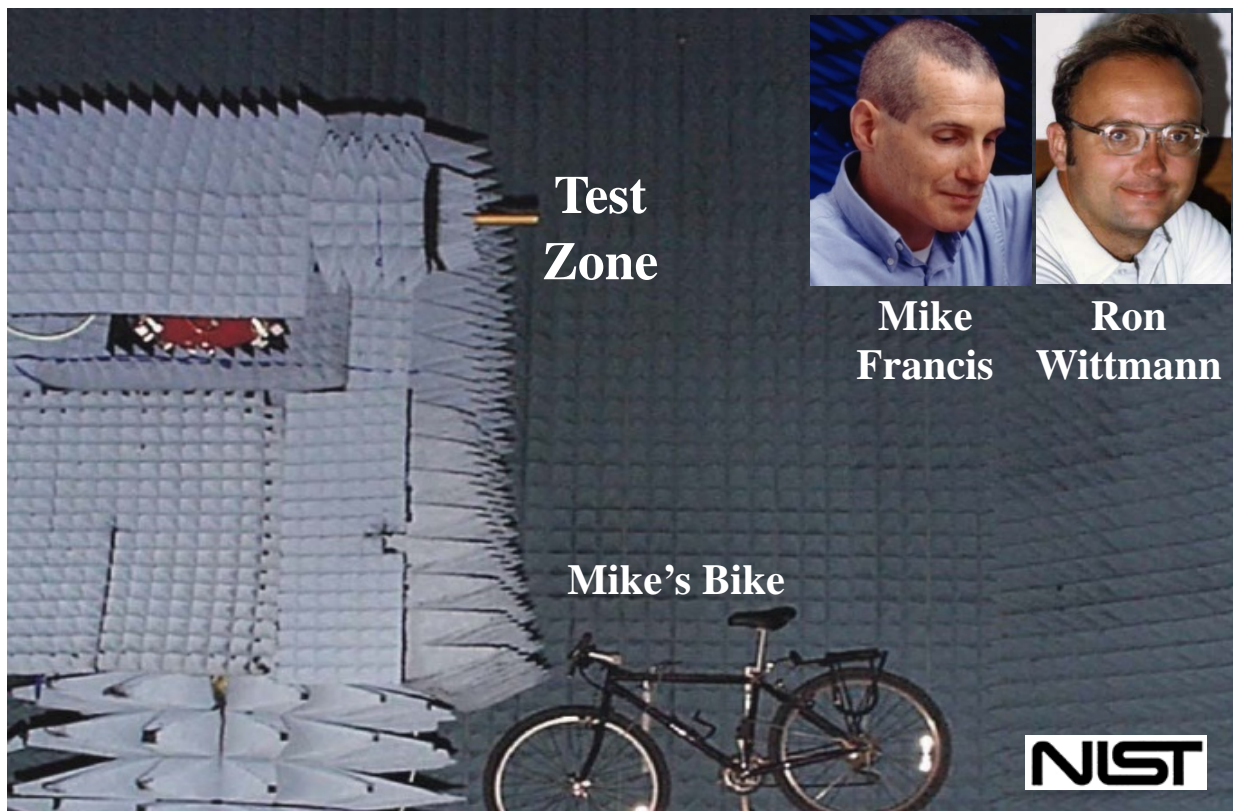


Figure 8. NIST Cylindrical/Spherical Near Field Range with Mike's Bike



Figure 9. Image of Mike Francis' bicycle made using the spherical mode spectra of the measured test-zone probe data taken on the test-zone sphere at the NIST Cylindrical/Spherical Near-field Range.

The Howland Company working with Ron Wittmann, Mike Francis, and Ed Joy became interested in the measurement of spherical test-zone fields in large anechoic chambers. Linear scanners to perform test-zone field measurements in large anechoic chambers are large, expensive and require large set up times. A spherical scanner, by comparison, might be less expensive and require smaller set up times. Figure 10 is a photo of a Howland Company 30ft diameter spherical test-zone scanner installed in a 70ft W x 40ft H x 110ft L anechoic chamber. The probe is dual polarized with a switch to switch between the two linearly polarized probe antennas. Figure 11 shows the image of the sources of the range test-zone fields. The primary source of the test-zone field is the range antenna, which is clearly identifiable. Walkway absorber and the back wall absorber reflections are also identifiable. The test-zone measurements were made at 1 GHz.

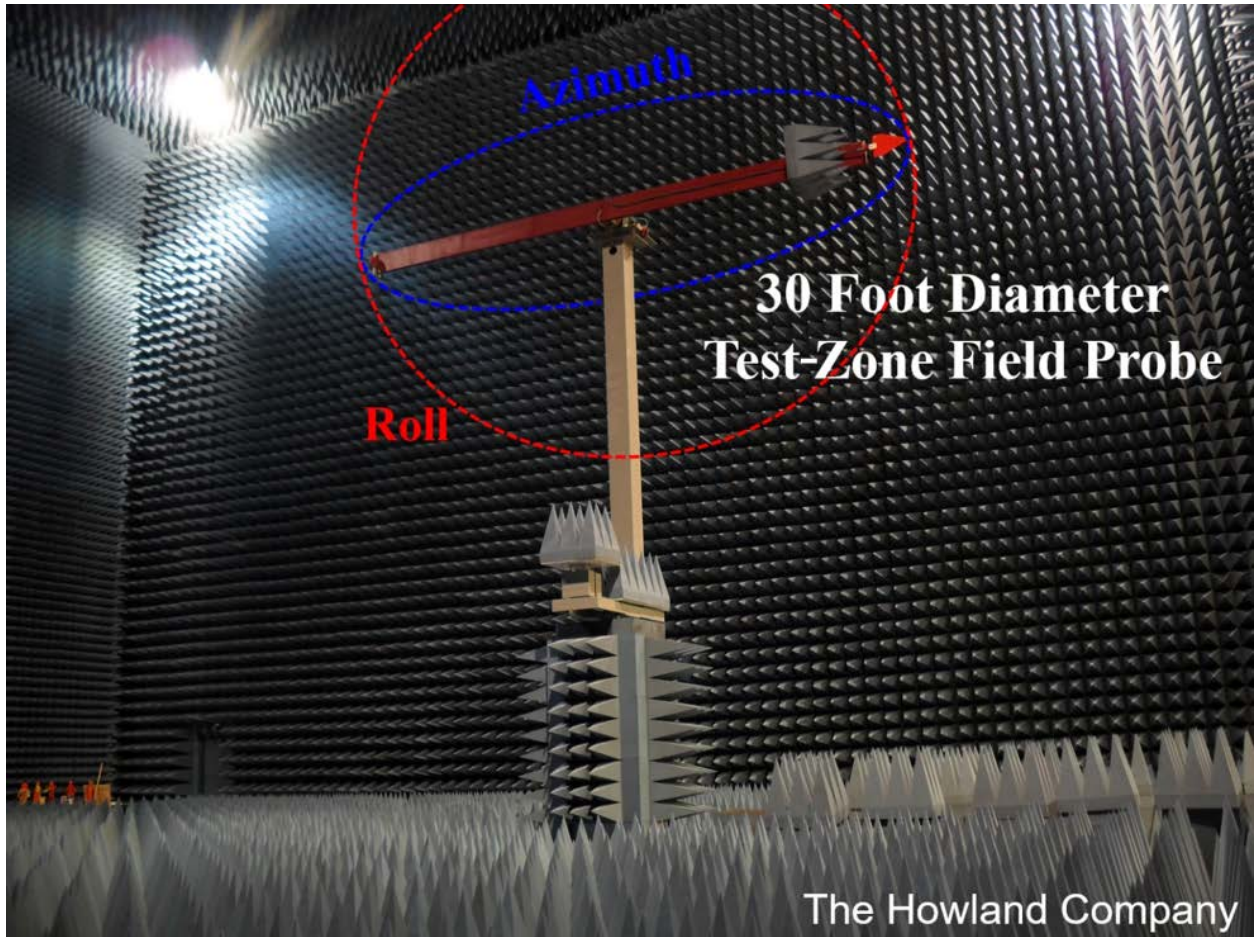


Figure 10. The Howland Company commercial spherical test-zone measurement system being used to measure the spherical test-zone field of a large anechoic chamber.

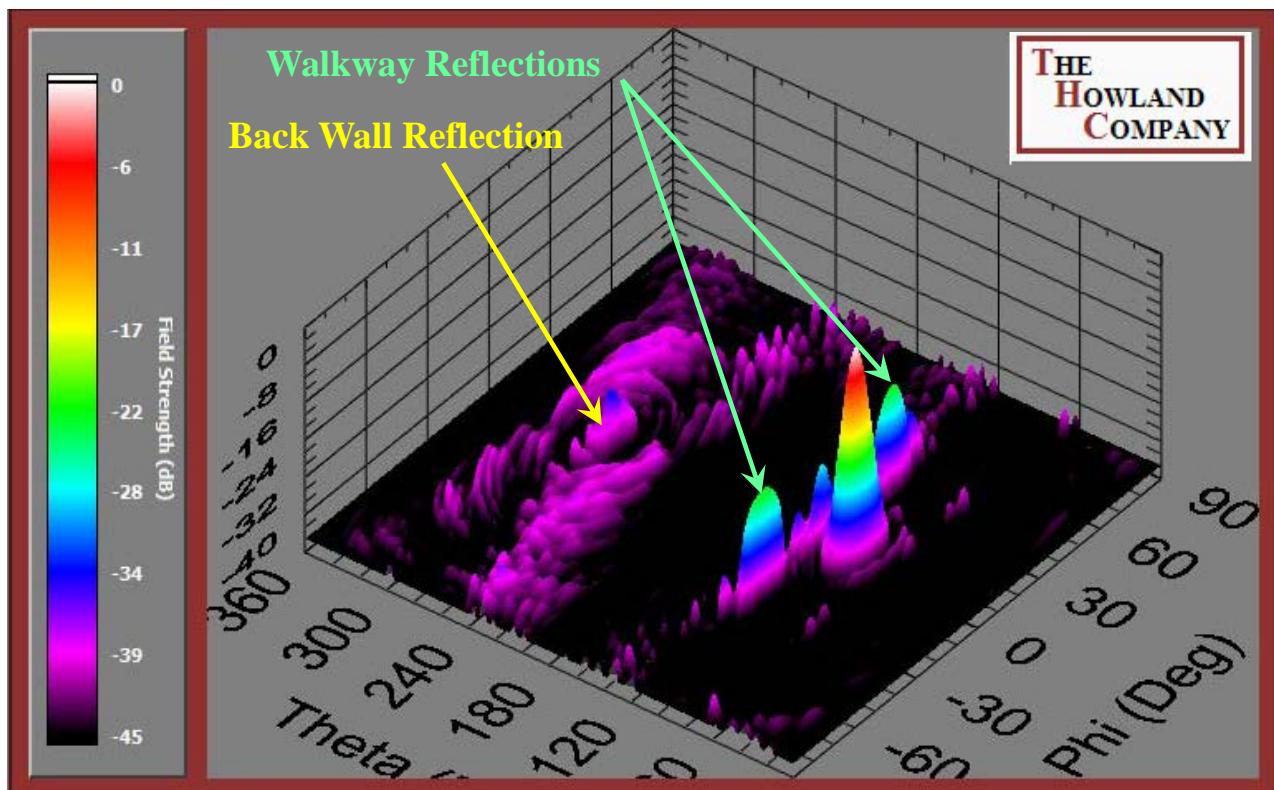


Figure 11. The Howland Company calculated image of the sources determined from the spherical modal spectrum of the measured spherical surface test-zone field. The 0 dB peak is the peak of the range antenna spherical mode spectrum. The range antenna is located at $\Theta = 90^\circ$, $\Phi = 0^\circ$. The back wall reflection is centered at $\Theta = 270^\circ$, $\Phi = 0^\circ$ with a peak reflectivity of approximately -34 dB at 1 GHz.

Compensation

The basic idea of compensation is to remove the effects of imperfections in the test-zone field, usually amplitude and phase taper and polarization effects of the range antenna, range reflections, and RF leakage from equipment. Range reflections originate from metallic objects in the range, such as cables, positioners, tools, fire sprinkler heads, ventilation ducts and lighting fixtures. Range reflections can also originate from missing, defective or undersized absorber and from supposedly invisible dielectric materials. The ideal solution is to select range antennas and range length to minimized range antenna imperfections, removal of all reflecting objects, and repair all RF leakages. Range characterization is used to

determine the quality of the range. The range characterization might identify still further reflectors or leakages which can be repaired. Range compensation is an option to further increase the quality of the range test-zone field.

Range compensation starts with an accurate measurement of all fields entering the empty test zone, the physical zone in space where an AUT will be placed for the measurement of its electromagnetic performance. The above presentation of range characterization addresses this first step of range compensation. Range characterization requires that the range antenna is energized and aligned for measurement of an AUT, but the AUT is not present. What is present is an apparatus for measuring the test-zone field. The measurement of the spherical test zone is followed by the calculation of the complex vector spherical mode angular spectrum of the test-zone field. The ideal test-zone field is a plane wave with uniform amplitude, phase and polarization where the perpendicular direction to the uniform amplitude and phase front points directly to the phase



Don Black

center of the range antenna. The direction to the range antenna is the reference direction for the two spherical angles of measurement, such as azimuth and elevation.

The ideal test zone is actually two ideal test zones. Each of the two ideal test-zone fields is a single linearly polarized plane wave: one vertically polarized and one horizontally polarized. Polarization of the spherical test zone is determined by performing two spherical test zone measurements for each orientation of the range antenna: A co-polar and a cross polar measurement. Thus, there are actually four spherical test zone measurements: Co-polar and cross-polar when the range antenna is vertically polarized and co-polar and cross-polar when the range antenna is horizontally polarized. The result is two complex vector test zone fields. The measured test-zone fields are usually not ideal plane waves. The unwanted parts of the measured test-zone fields are the parts that differ from the two ideal plane wave fields. The next step in range compensation is the measurement of an AUT in the characterized two test zones. The AUT is rotated to each spherical sampling direction, specified by the sampling criteria for the AUT. The results of the interaction of the AUT with the test-zone fields at each angle of AUT rotation is a

single complex quantity, which is measured. The AUT is rotated, the test zone is not rotated. Combining the two measurements results in a measured complex vector response of the AUT, where the variables are the two angles of spherical AUT rotation. What is known is the complex vector spherical mode spectrum of the test-zone fields, the complex vector far-field pattern of the probe and the measured complex AUT responses to the test-zone fields, which contain the effects of the extraneous fields of the test zone. What is unknown is the complex vector spherical mode spectra of the AUT.

Don Black was able to solve for the unknown AUT complex vector spherical mode spectrum. The solution for the AUT spherical mode spectrum, which effectively removes the effects of the extraneous test-zone fields. Details of this calculation can be found in his dissertation and several papers. The computations required in this spherical mode spectra model, however, are quite intensive and time consuming. Don demonstrated that range compensation really works.

The reflectivity level of the Georgia Tech Spherical Near-field/Far-field Range is -35 to -40 dB with respect to the 0 dB level of the main beam peak of the AUT under typical measurement conditions at X-band. Figure 12 shows the plane wave spectrum of the test-zone field, which was fitted to the spherical mode spectrum of the test-zone field, of the Georgia Tech Spherical Near-field/Far-field Range. The range has been outfitted with two reflectors and a variable extraneous source. The extraneous source is a small horn antenna. The range RF source output is split with most of the power directed to the range antenna and a smaller variable level of power directed to the extraneous source small horn. Considering the level of power directed to the small horn and the relative gain of the small horn as compared to the gain of the range antenna, the test-zone field level produced by the small horn is approximately -20 dB, in this case, as compared to the range antenna main beam peak level of 0 dB.

The range test-zone spectrum includes the angular spectrum of the range antenna with its wide angular base and a collection of narrow spikes of radiation. The wide angular base of the range antenna spectrum is the result of test-zone amplitude and phase tapers due to the finite distance from the range antenna to the test zone. The narrow spikes are due to the two range reflectors and an extraneous source. The narrow angular spectrum of the spikes resembles the spectrum of plane waves, each of the plane waves would have a very narrow angular spectrum.

Perhaps the model of the test-zone field should be a collection of plane waves, each with a unique amplitude, phase and polarization and direction of arrival into the test zone.

Daniel Leatherwood thought that the multiple plane wave model was a good idea and began a new model of the test-zone field. His idea was to measure and model the spherical test-zone fields as usual and express the measurements in spherical mode expansions exactly like Don Black had done. The new idea was to fit the spherical mode expansion with a finite number of plane waves, each plane wave with its own amplitude, phase and polarization and with its own direction. Part of the fitting plane waves to the spherical mode expansion is the ability to only use plane waves above a certain, selectable amplitude level. This greatly reduces the number of plane waves and does not try to represent noise level amplitudes with plane waves. The fitting of the plane waves to the spherical modal spectrum was a major part of Daniel's research. Daniel was able to calculate a complex vector plane-wave spectrum of the test-zone field from the complex vector spherical mode spectrum of the test-zone field. The extra computational step of fitting plane waves allowed rapid plane wave test-zone field compensation as compared to an all spherical mode compensation, more than making up for the extra computational time. Details of this calculation can be found in his dissertation and several papers.

Each test-zone plane wave can be thought of as an ideal test-zone field. Should an AUT be measured in an ideal plane wave test zone, the measurement would yield the true far-field pattern of the AUT.

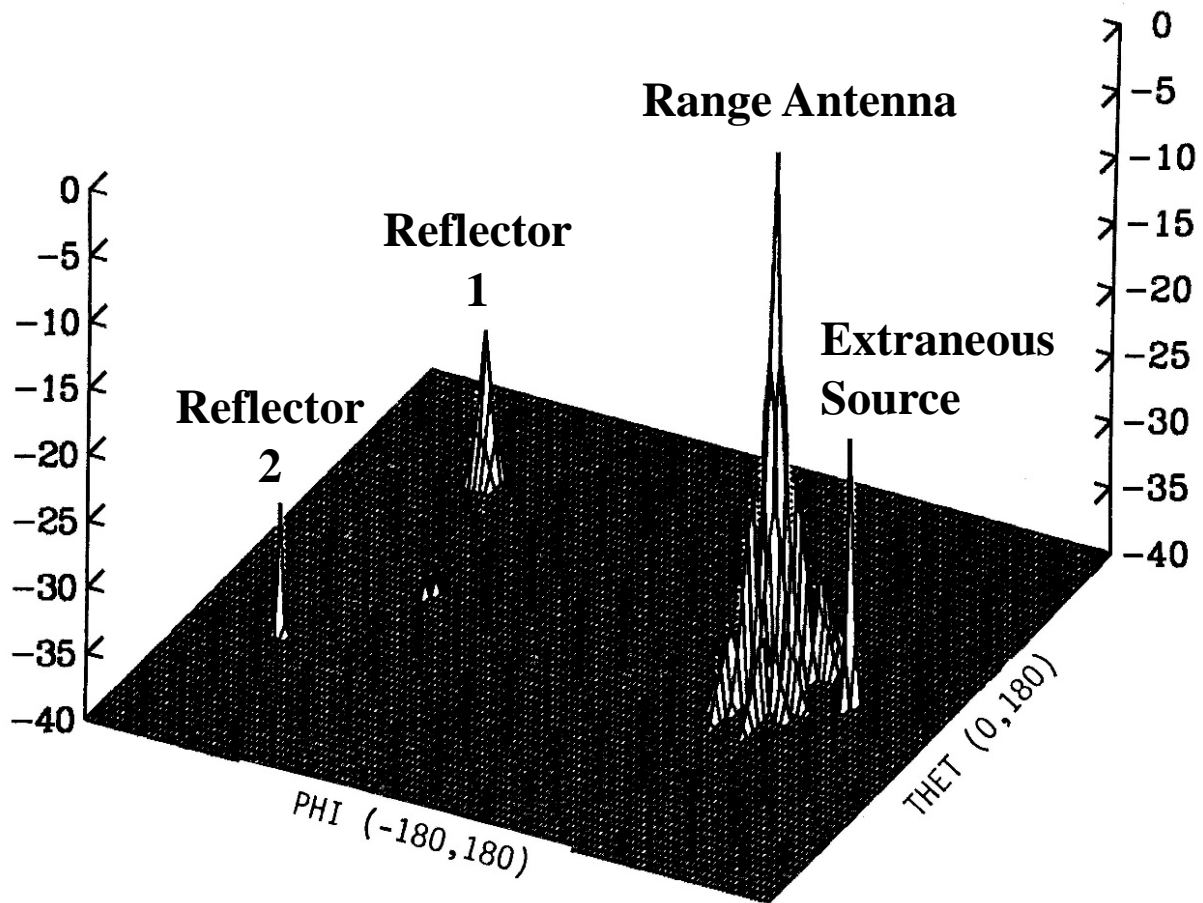


Figure 12. Amplitude in dB of the test-zone plane wave spectrum measured at 9.33 GHz, showing the spectra of the range antenna, two range reflections and an extraneous source.

Figure 12 shows the range antenna located at theta (roll) = 90° and phi (azimuth) = $+90^\circ$ and the extraneous source is located at theta (roll) = 90° and phi (azimuth) = 60° in this case. The plane wave spectrum amplitude has been normalized to 0 dB at the peak of the range antenna spectrum and the extraneous source has a magnitude of approximately -20 dB in this case.

The AUT pattern measured in a spherical test zone where the spherical test zone is modeled as collection of M plane waves is given by:

Measured Pattern = Pattern of AUT Due to the Range Antenna Plane Wave ($m = 0$) + Sum of AUT Patterns Due to Each Extraneous Plane Wave, $m = 1, 2, 3, \dots, (M-1)$

Each plane wave in the test zone is viewed as being created by a perfect range antenna located at great distance from the test zone. Each plane wave produces an accurate measurement of the AUT pattern, however the pattern amplitude is changed to the complex vector amplitude of the plane wave and rotated to the angle of the plane wave arrival. If there are 50 plane waves in the test-zone model, a spherical measurement of the AUT will produce $M = 50$ accurate AUT far-field patterns added together. Compensation is then finding a way to keep one pattern, $m = 0$, the one measured by the range antenna plane wave, and subtracting the other $M-1$ patterns measured by the $M-1$ extraneous plane waves.

Daniel found an iterative solution for the compensation. An estimated pattern is calculated and then updated on each iteration, n , as follows:

$$\begin{aligned} \text{Estimated Pattern}_n &= \text{Measured Pattern}_0 \\ &- \text{Sum of Estimated AUT Patterns}_{n-1, m} \end{aligned}$$

**One for Each Extraneous Plane Wave, $m = 1, 2, 3, \dots (M-1)$
for Iterations $n = 1, 2, 3, \dots$**

The latest iteration Estimated Pattern _{n} , equals the one and only Measured Pattern _{0} (the pattern which includes the effect of the range antenna and all the extraneous fields in the test zone) minus the sum of the Estimated AUT Patterns due to each extraneous plane wave ($1 < m < M-1$). The complex vector amplitude and the direction of propagation into the test zone for each extraneous plane wave is known from range characterization. The true pattern is unknown, so the latest estimated pattern _{n} is used as the latest estimation of the true pattern. It is very important that the actual measurement of the AUT, measured pattern _{0} , is never changed in the iteration. Measured pattern _{0} is actually estimated pattern _{0} . This is the rock of stability for the iteration. The first iteration produces the first estimated pattern _{1} which equals the measured pattern _{0} minus the extraneous patterns _{$1,m$} . The

extraneous patterns $s_{l,m}$ are amplitude, phase and polarization weighted by the complex vector value of each extraneous plane wave and thus are much lower in amplitude; think range reflection levels of -20 dB, -30 dB, -40 dB, etc. The major errors in the measured pattern p_0 are due to the measurements of the true pattern main beam as it is rotated to the directions of each of the extraneous plane waves. There is a large increase of pattern measurement accuracy after this first iteration. Daniel showed that the maximum reflectivity level of the range is reduced by the maximum level of all extraneous fields multiplied by the iteration number. With a maximum extraneous level of -20 dB, after one iteration the maximum extraneous field level is -40 dB. Very few iterations are normally required.

Most of the computation time of compensation (after the computation of the spherical mode spectrum of two spherical test-zone fields) is interpolation of the AUT estimated patterns as the AUT patterns are rotated in azimuth and elevation to the angular location of each extraneous plane wave and added to the current total of estimated patterns. The interpolations are complex vector interpolations. Figure 13 shows the spherical coordinate system of the AUT measurement sphere A and rotated version S. Note the phi and theta rotations produce different interpolation requirements. Daniel investigated and found that Bivariate 3 x 3 Lagrange interpolation produced the best results.

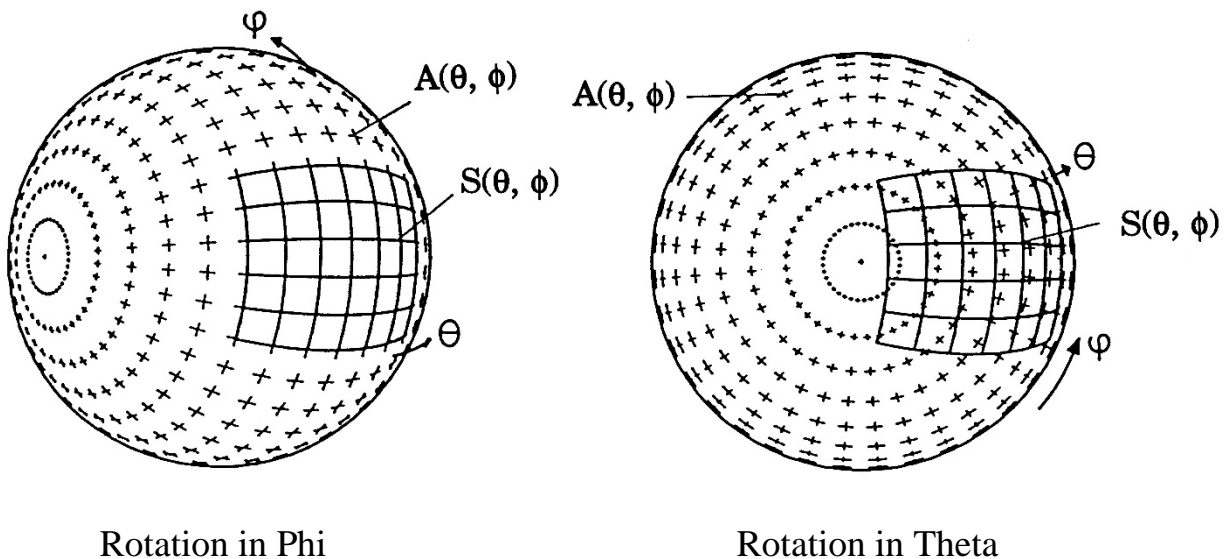


Figure 13. Comparison of the rotated, A, and unrotated, S, AUT estimated pattern polar coordinate system with estimated pattern rotation in theta = azimuth and

$\phi = \text{roll}$.

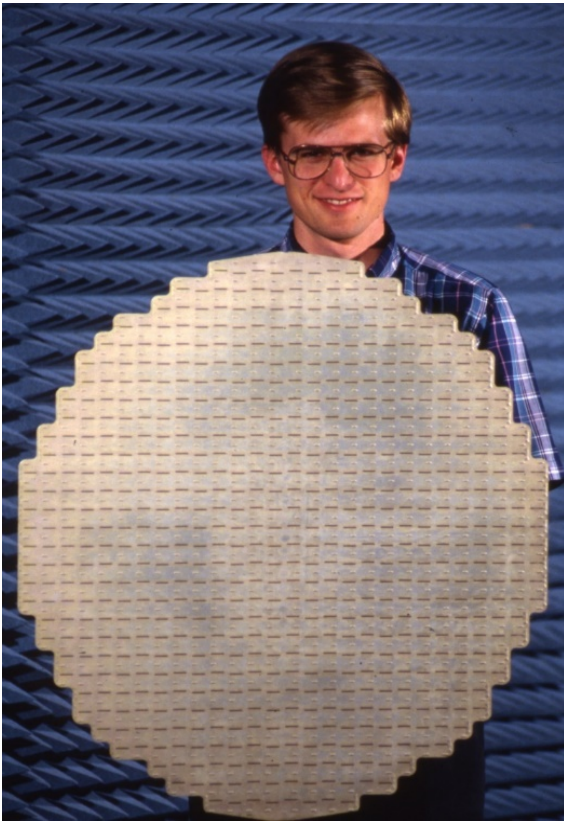


Figure 14. Daniel Leatherwood holding the 474 slotted-waveguide-element planar array AUT. The antenna has a 71.7 cm x 65.26 cm elliptical aperture and operates at 9.33 GHz with approximately -25 dB peak sidelobe level.

The simplest demonstration of range compensation using only one extraneous field was undertaken. The extraneous field is designed to be controllable in amplitude. The range antenna pattern and finite distance from the test zone produce amplitude and phase taper errors, which are also included. The AUT shown in Figure 14 is a flat-plate, fixed-phased array operating at 9.33 GHz. Figure 15 shows the arrangement for the spherical surface measurement of the AUT. Figure 15 shows the array antenna AUT on a polar, roll over azimuth positioner, the range antenna and the extraneous source antenna located 20° in azimuth. The AUT, range antenna and extraneous source are in a horizontal plane. Prior to AUT measurement the spherical test-zone field was measured.

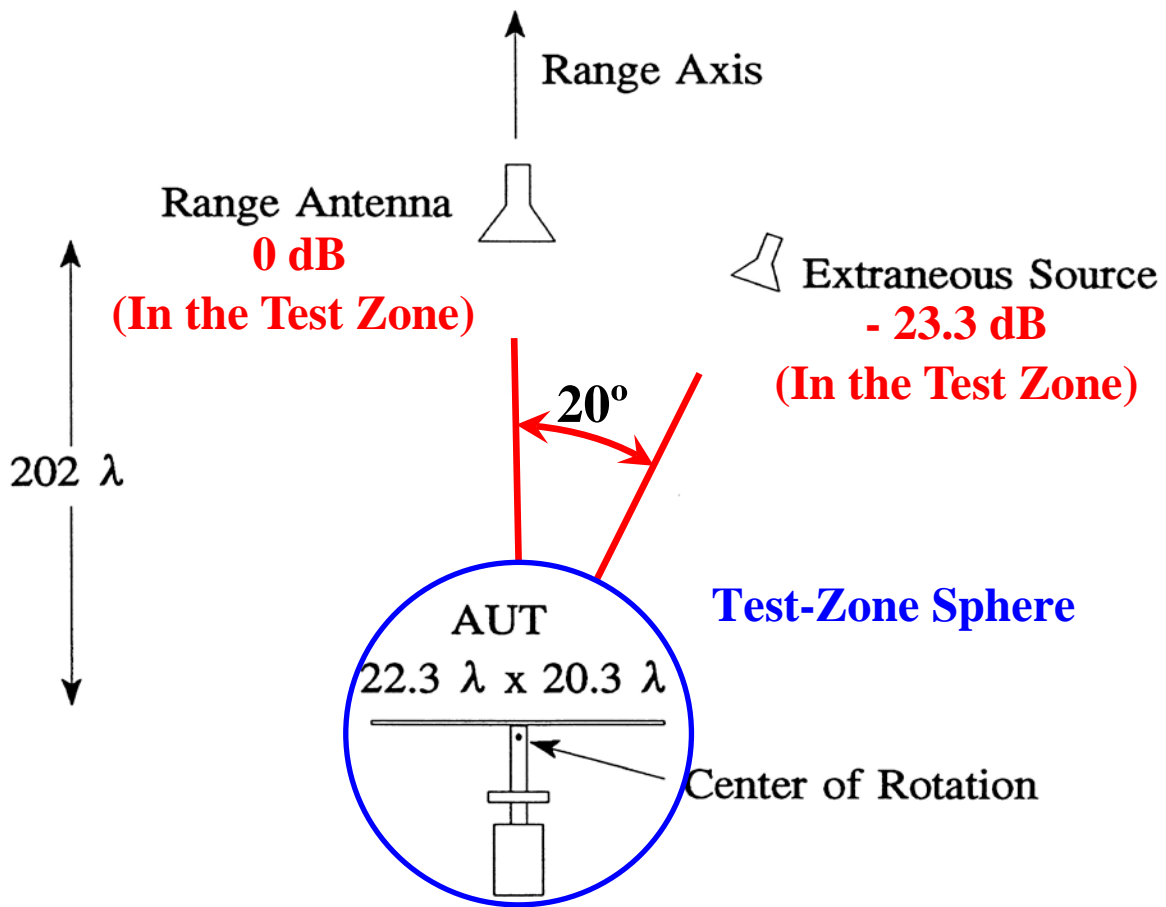


Figure 15. Range configuration showing range antenna, AUT and single extraneous source with -23.3 dB excitation relative to the 0 dB range antenna excitation, all located in the horizontal plane

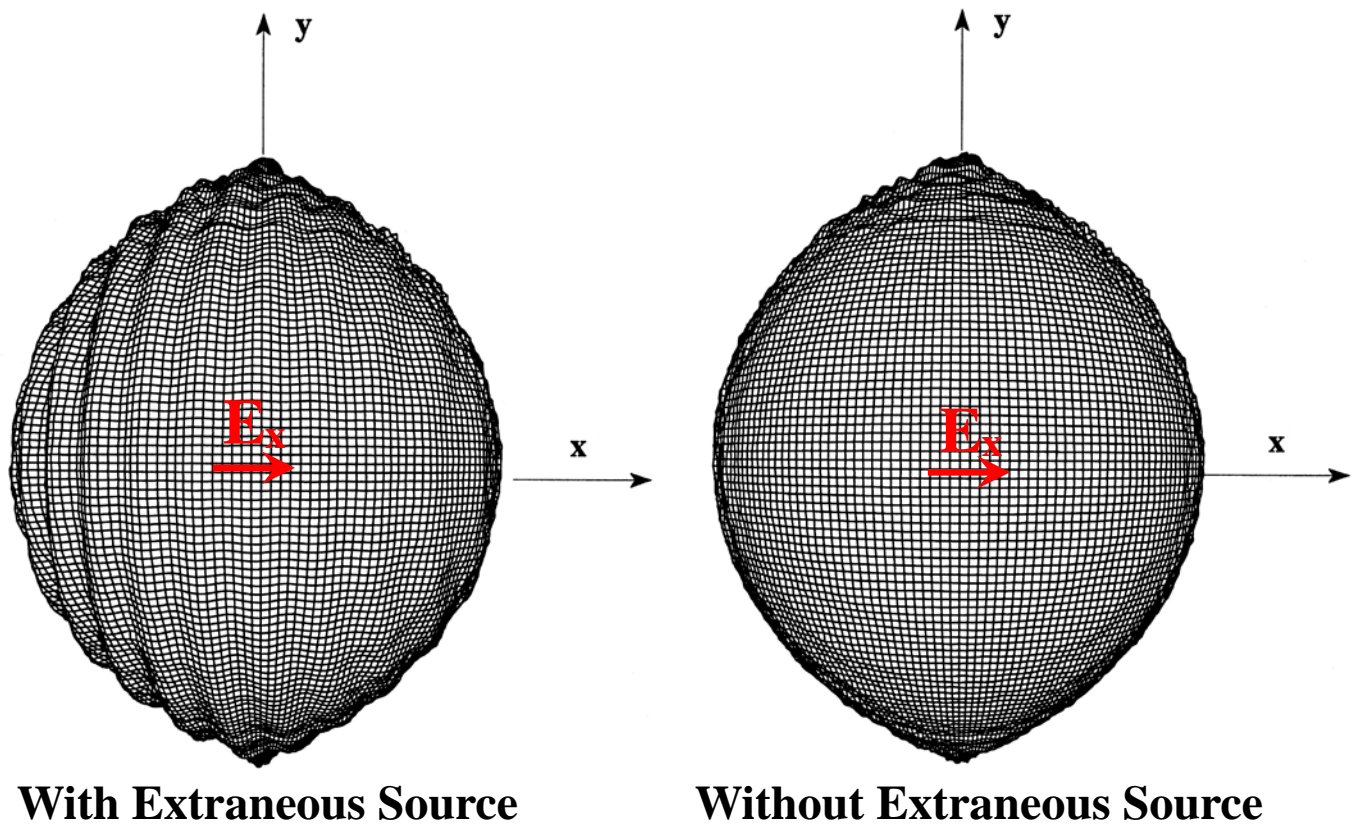


Figure 16 shows the measurement of the spherical test-zone field horizontal component amplitude, E_x , with and without the single extraneous source activated. The effect of the extraneous source is clearly visible. The cross-polar field, E_y , not shown, had a peak amplitude of approximately -30 dB in both cases.

Figure 17 shows the measured patterns of the flat-plate array with and without the extraneous source activated. The amplitude scale is -70 dB. Daniel spent a lot of time upgrading the dynamic range of our spherical range, including developing an amplitude and phase drift correction technique and mechanically realigning the positioners.

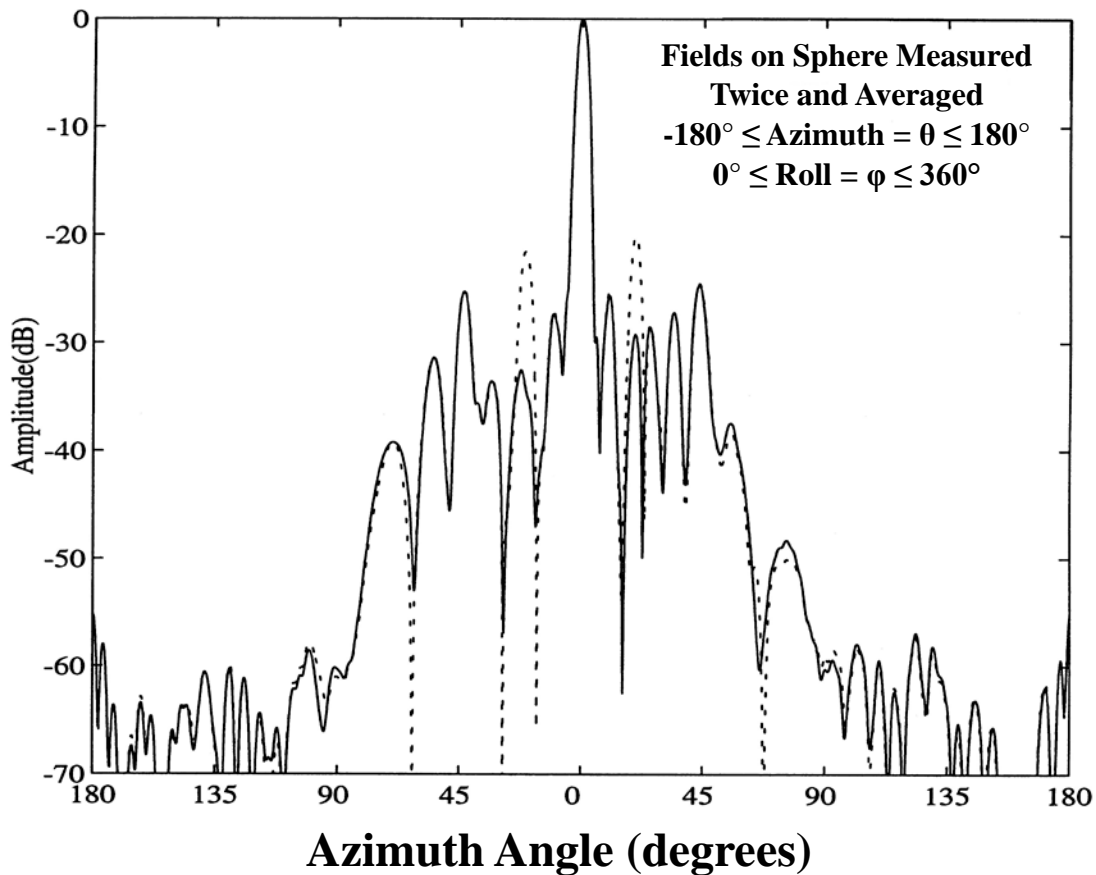


Figure 17. Azimuth far-field pattern azimuth cut of the flat-plate array AUT with (dotted line) and without (solid line) the extraneous source activated

It is important to understand the technique of measuring the sphere twice: $-180^\circ \leq \text{azimuth} = \theta \leq 180^\circ$ and $0^\circ \leq \text{roll} = \varphi \leq 360^\circ$. There is a mechanical advantage of keeping big and heavy things moving at a constant rate, as starting and stopping produces uneven rotation and induces vibration. The azimuth positioner is the big and heavy thing. The roll positioner, by comparison, is much smaller and much lighter. The technique used to minimize stopping and starting is to increment the roll positioner one roll positioner angular spacing, which involves starting and stopping the roll positioner, as the moving azimuth rotator passes through the region of azimuth angles near 180° . The 180° region is where the roll positioner blocks the rear radiation of the AUT. Thus, this part of the pattern is measured with much lower accuracy. This region is approximately 20° wide in azimuth. The benefit is that the big and heavy azimuth rotator does not need to be stopped or started. The time required for the azimuth positioner to pass through

the approximately 20° region is long enough for the roll positioner to start and stop, and vibrations to dampen out.

A roll angle of 0° corresponds to the horizontal (right-side-up) orientation of the AUT, a 180° roll orientation corresponds to an upside-down orientation of the AUT. Should the measurement continue going beyond a 180° roll for another 180° , while continuing to rotate in azimuth, the AUT sphere will be measured twice, with different angular parts of the AUT pattern exposed to different angular parts of the range. One sphere measures a right-side-up AUT and the other sphere measures and upside-down AUT. The average of these two patterns, statistically, is better than either one. When the AUT is upside-down, azimuth is really negative azimuth. This fact must be taken into account when averaging and when viewing the azimuth patterns. The single extraneous source in Figure 15 is seen to produce two extraneous peaks (a + azimuth peak and a - azimuth peak) as seen in Figure 17 due to the averaging of the two spherical patterns in this manner.

Figure 18 shows the results of three iterations of the plane wave subtraction compensation technique. More iterations have negligible effect. Remnants of the extraneous source remain, but at greatly reduced values.

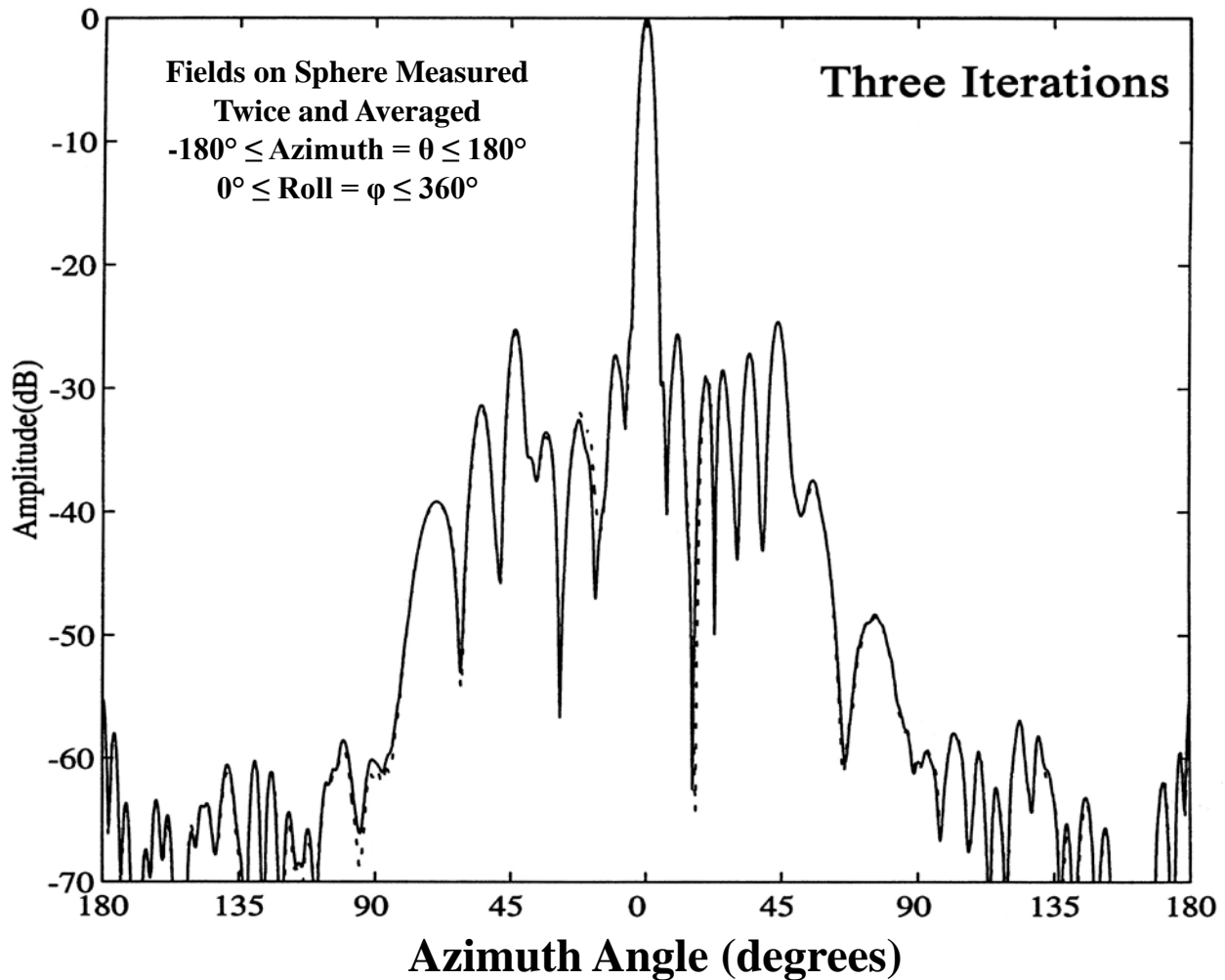


Figure 18. Azimuth far-field pattern cut of the flat-plate array AUT without extraneous source (solid line) and with compensated extraneous source (dotted line) after three iterations of plane wave pattern subtraction compensation.

Figure 19 shows the azimuth cut of the plane wave error spectrum of the AUT measurement. Compared is the direct measurement of the extraneous source by the AUT with the range antenna not active as compared to the compensation algorithm prediction of the extraneous-source-only AUT measurement. Note that the error in the measurement of the AUT main beam located at Azimuth = 0° is very small.

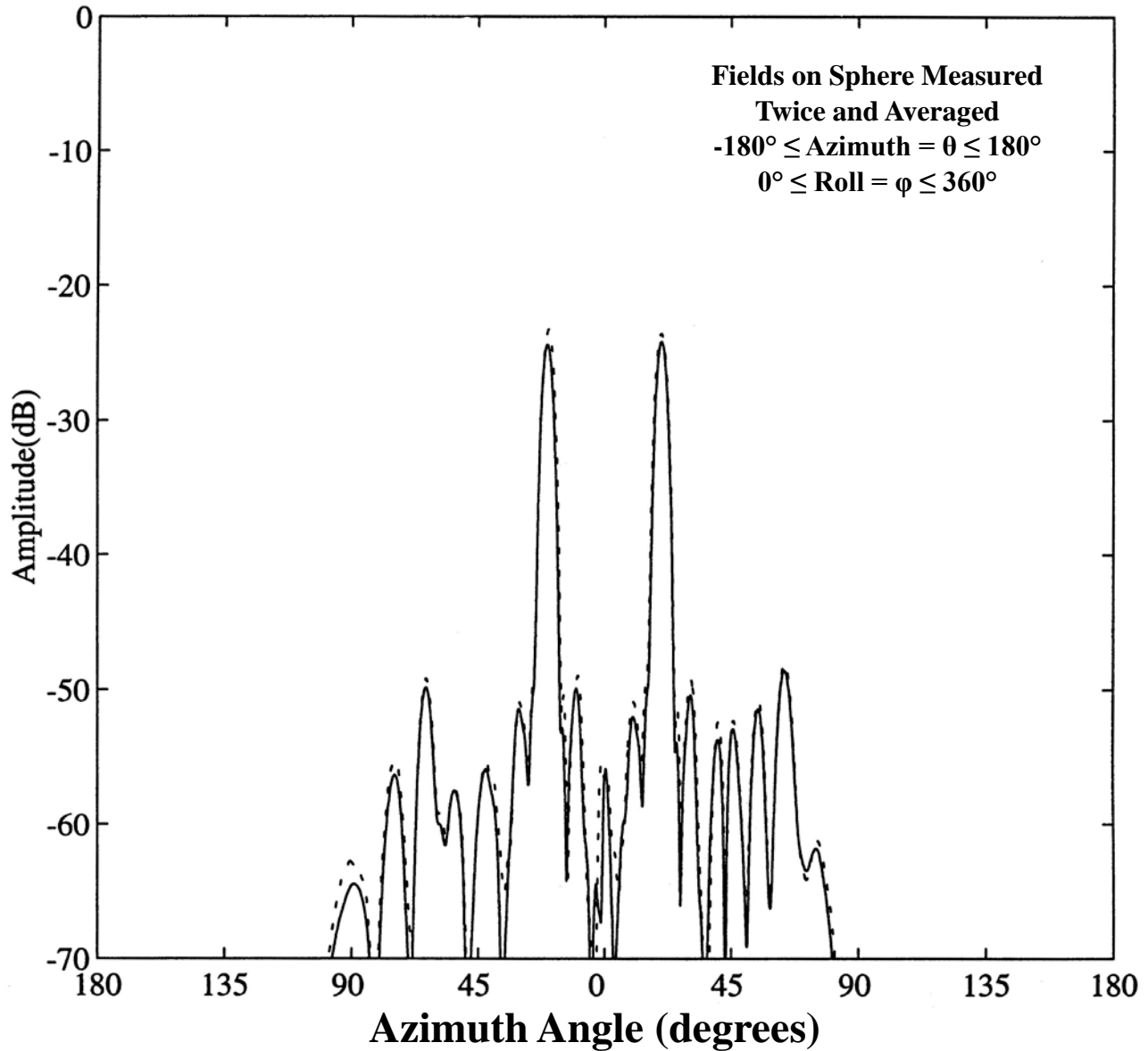


Figure 19. Azimuth far-field pattern cut of the flat-plate array with extraneous source active and the range antenna source inactive (solid line) and the calculated error due to the extraneous source (dotted line) after three iterations of pattern compensation.

Range characterization and compensation is a practical technique for improving the accuracy of antenna measurements on fixed line-of-site antenna measurement facilities. It has been theoretically developed, implemented and demonstrated. The required additional equipment necessary to perform the spherical probing of the test zone is modest. The technique requires the measurements be taken at only one measurement frequency. The demonstration showed that the reflectivity level after three iterations of compensation is approximately $3 \times (-23.3 \text{ dB}) = -69.9 \text{ dB}$. Spherical test-zone field compensation does not reduce antenna pattern measurement errors to zero. It attempts to greatly reduce the effects of imperfections in the test-zone field. These imperfections include amplitude, phase and polarization errors due to the range antenna and range geometry and reflections for various objects in and around the range. It does not attempt to reduce instrumentation errors, positioning errors or random errors.

The Georgia Tech research was a team effort spanning 1987-1998. The team was composed of Don Black, Daniel Leatherwood, Mike Guler, Richard Wilson and Ed Joy. Professor Luis Jofre, Technical University of Catalonia, Barcelona, Spain (during his sabbatical at Georgia Tech) was instrumental at the early stages of this research.

Follow on Research

Randy Direen, Mike Francis and Ron Wittmann at NIST in Boulder advanced range characterization with imaging, as shown in this remembrance.

Carl Sirles, John Mantovani, Ray Howland, and Jim Hart, of The Howland Company, produced commercially available spherical test-zone measurement equipment and software.

Doren Hess of MI Technologies developed IsoFilter™, a way to apply angular spectrum filtering to an AUT measurements and “filter out” extraneous fields.

Greg Hindman of NSI together with Allen Newell of NIST and NSI developed a similar technique, MARS™, Mathematical Absorber Reflection Suppression, to apply spherical spectrum mode filtering to AUT measurements to “filter out = absorb” extraneous fields.

Scott Goodman and Robert Burkholder of The Ohio State University developed Range Transfer Function and Deconvolution using plane waves to reduce range reflections.

Sponsors

Thank you to our sponsors who supported this work:

Joint Services Electronics Program

Scientific-Atlanta

National Science Foundation

Department of Defense (AASERT Program)

References

- L. Jofre, E. B. Joy, and R. E. Wilson, "Antenna Pattern Correction for Range Reflections," in *Proc. 1987 Antenna Measurement Techniques Association Meeting*, Seattle, Washington, pp. 63-68, September 28-October 2, 1987.
- M. G. Guler, E. B. Joy, and D. N. Black, "Planar Surface Near Field Data Determined from Spherical Surface Near Field Measurements," in *Proc. 1989 Antenna Measurement Techniques Association Meeting*, Monterey, California, pp. 14-9 through 14-12, October 9-13, 1989.
- R. C. Wittmann, "Spherical Near-field Scanning: Determining the Incident Field Near a Rotatable Probe," *Antennas and Propagation Symposium Digest*, pp. 224-227, Dallas, TX, 1990.
- D. N. Black and E. B. Joy, "Spherical Probing of Spherical Ranges," in *Proc. 1990 Antenna Measurement Techniques Association Meeting*, Philadelphia, Pennsylvania, pp. 14-19 through 14-24, October 8-11, 1990.
- R. E. Wilson, D. N. Black, E. B. Joy, M. G. Guler, and G. Eder, "Spherical Probing Demonstrated on a Far-field Range," in *Proc. 1991 Antenna Measurement Techniques Association Meeting*, Boulder, Colorado, pp. 10A, 15-21, October 7-11, 1991.
- D. N. Black, E. B. Joy, M. G. Guler, and R. E. Wilson, "Extraneous Field Source Detection Using an Enhanced Spherical Probing Technique," in *Proc. 1992 Antenna Measurement Techniques Association Meeting*, Columbus, Ohio, pp. 7-16 through 7-21, October 19-23, 1992.
- R. E. Wilson, D. N. Black, E. B. Joy, and M. G. Guler, "Generating Linear Probing Data from Spherical Probing Data," in *Proc. 1992 Antenna Measurement Technique Association Meeting*, Columbus, Ohio, pp. 7-22 through 7-26, October 19-23, 1992.
- D. N. Black, E. B. Joy, J. W. Epple, M. G. Guler, and R. E. Wilson, "The Effect of Spherical Measurement Surface Size on the Accuracy of Test-Zone Field

- Predictions,” in *Proc. 15th Annual Meeting and Symposium of the Antenna Measurement Techniques Association*, Dallas, Texas, pp. 239-243, October 4-8, 1993.
- D. N. Black, E. B. Joy, D. A. Leatherwood, and R. E. Wilson, "Demonstration of Test-Zone Field Compensation in an Anechoic Chamber, Far-field Range," in *Proc. 16th Annual Meeting and Symposium of the Antenna Measurement Techniques Association*, Long Beach, California, pp. 194-199, October 2-7, 1994.
- D. N. Black, "Test-Zone Field Compensation," PhD Dissertation, Georgia Institute of Technology, Atlanta, GA, USA, 1995
- D. N. Black and E. B. Joy, "Test-Zone Field Compensation," *IEEE Trans. Antennas and Propagation*, vol. 43, no. 4, pp 362-368, April 1995.
- R. C. Wittmann and D. N. Black, "Antenna/RCS Range Evaluation Using a Spherical Synthetic-Aperture Radar," in *Proc. 18th Annual Meeting and Symposium of the Antenna Measurement Techniques Association*, Seattle, Washington, pp. 406-410, September 30 – October 3, 1996.
- D. A. Leatherwood and E. B. Joy, "Range-Field Plane Wave Model Determined From Spherical Probing Data," in *Proc. 19th Annual Meeting and Symposium of the Antenna Measurement Techniques Association*, Boston, Massachusetts, pp.170-175, November 17-21, 1997.
- D. A. Leatherwood and E. B. Joy, "Plane Wave, Pattern Subtraction, Range Compensation for Spherical Surface Antenna Pattern Measurements," in *Proc. 19th Annual Meeting and Symposium of the Antenna Measurement Techniques Association*, Boston, Massachusetts, pp. 199-204, November 17-21, 1997.
- D. A. Leatherwood, "Plane Wave, Pattern Subtraction, Range Compensation," PhD Dissertation, Georgia Institute of Technology, Atlanta, GA, USA, 1998.
- D. A. Leatherwood and E. B. Joy, "Demonstration of Plane Wave, Pattern Subtraction, Range Compensation," in *Proc. 20th Annual Meeting and Symposium of the Antenna Measurement Techniques Association*, Montreal, Quebec, Canada, October 26-30, 1998.
- R. C. Wittmann and M. H. Francis, "Test-Chamber Imaging Using Spherical Near-Field Scanning," in *Proc. Antenna Meas. Tech. Assoc.*, pp. 87-91, Oct. 2001.
- D. A. Leatherwood and E. B. Joy, "Plane Wave, Pattern Subtraction, Range Compensation," *IEEE Transactions on Antennas and Propagation*, December 2001.
- R. H. Direen, M. H. Francis and R. C. Wittmann, "Near-field spherical scanning: Test-zone field evaluations," in *Proc. 3rd European Conference on Antennas and Propagation*, pp. 2921-2924, Mar. 23-27, 2009.
- C. W. Sirles, J. C. Mantovani, A. R. Howland, B. J. Hart, Anechoic Chamber

Performance Characterization Using Spherical Near-Field Imaging Techniques,
Proc. 3rd European Conference on Antennas and Propagation, 2009.

R. H. Direen, M. H. Francis and R. C. Wittmann, “Near-field spherical scanning:
Test-zone field evaluations,” in *Proc. Antenna Meas. Tech. Assoc.*, pp. 126-
129, Nov. 1-6, 2009.